Mascot/CAM

MASCOT
Mobile Asteroid Surface Scout

]

Document Approval Sheet

Document title:	**MASCam PDS Archive Software Interface Specification**
Document number:	MSC-DLRPF-SP-XXX
Issue:	0
Revision:	1
Date of Rev.:	16.02.2023
File name:	MASCOT-MASCam-DLR-SIS_230216.docx

Prepared by:	.... (name of author(s))	Date:
Released by:	.... (name of Work Package leader)	Date:
Approved by:	.... (name of project leader)	Date:

Table of Contents

List of Acronyms

ADC	Analogue/Digital Converter PCB
ADJ	Adjustment devices
CAM	Mascot Camera
CH	Camera Housing
CHB	Camera Housing Back
CHF	Camera Housing Front
COTS	Commercial Off-The-Shelf
CTR	Controller PCB
DLR	German Aerospace Center
FPA	Focal Plane Assembly PCB
ID	Illumination Device
IF	Interface PCB
IFL	Infinity front lens
MOBT	Mascot On-Board Time
PCB	Printed Circuit Board
PL	Payload
SBN	Small Bodies Node

1 Documents

1.1 Applicable Documents

[1] Planetary Data System Standards Reference, Version 1.11.1.0, May 1, 2019.

[2] Planetary Science Data Dictionary Document, Version 1.11.1.0, May 1, 2019.

[3] Planetary Data System (PDS) PDS4 Information Model Specification, Version 1.11.1.0, May 1, 2019.

[4] "Open VICAR", http://www-mipl.jpl.nasa.gov/vicar_open.html

The PDS4 documents [1] through [3] are subject to revision. The most recent versions may be found at pds.nasa.gov/pds4.

1.2 Reference Documents

[5] Preusker, F., et al., The MASCOT landing area on Asteroid (162173) Ryugu, Astronomy & Astrophysics 632 (2019). doi:10.1051/0004-6361/201936760.

[6] Biele, J.; Fischer H.-H., MASCOT Time Scales, MCS-TN-1053_Time_Scales, DLR MUSC, urn: jaxa:darts:hayabusa2.mascam:document:mcs_tn_1053_time_scales

[7] Schroeder, S., MASCOT CAM On-Asteroid Activities, DLR PF, urn: jaxa:darts:hayabusa2.mascam:document:mascam_on_asteroid_phase

[8] Jaumann *et al*. (2016) "The Camera of the MASCOT Asteroid Lander on Board Hayabusa 2", Space Sci Rev 208, 375-400, doi:10.1007/s11214-016-0263-2

[9] Scholten *et al*. (2019) "The Hayabusa2 lander MASCOT on the surface of asteroid (162173) Ryugu – Stereo-photogrammetric analysis of MASCam image data", Astronomy & Astrophysics, 632, L5. EDP Sciences. doi: 10.1051/0004-6361/201936760

[10] Schroeder, S., *et al.*, Spectrophotometric analysis of the Ryugu rock seen by mascot: Searching for a carbonaceous chondrite analog, Planetary Science Journal (2021), doi: 10.3847/PSJ/abbb97

2 Introduction

2.1 Purpose and Scope

The purpose of this Software Interface Specification (SIS) document is to provide users of the MASCOT CAM (abbr. MASCam) archive with a detailed description of the data products and how they are generated, along with a description of the PDS4 archive bundle, the structure in which the data products, documentation, and supporting material are stored. The users for whom this document is intended are the scientists who will analyze the data, including those associated with the project and those in the general planetary science community.

2.2 MASCam Description

2.2.1 Science Objectives

The MasCam will provide the ground truth for the orbiter remote sensing observations. In addition, it will provide context for measurements by the other lander instruments (radiometer, spectrometer, and magnetometer), and the orbiter sampling experiment. By imaging dur- ing descent and on the surface, it will characterize the geological context, mineralogy and physical properties of the surface (e.g. rock and regolith particle size distributions). During day, clear filter images will be acquired. During night, illumination of the dark surface will be realized by four arrays of monochromatic light emitting diodes working in four spectral bands to allow identifying spectral variations on the surface. Continued imaging during the surface phase and image series at different sun angles over the course of an asteroid day will also contribute to the physical characterization of the asteroid surface properties by time-dependent photometric measurements of the regolith.

MasCam will contribute to the determination of the structural, textural and compositional characteristics of the surface layer by means of panchromatic and multi-color imaging of the asteroid surface on scale lengths ranging from tens of meters to a fraction of a millimeter. MasCam will operate as descent and in-situ imager (both during day and night phases). During descent, imaging will start shortly after the separation from the Hayabusa 2 mother spacecraft. Descent images will be acquired until touchdown of MASCOT. The images will close the resolution gap between orbital and surface imaging and allow to identify the land- ing site within the orbiter camera dataset. After touchdown, the camera will acquire wide- angle images of the asteroid's surface. From these images, surface features will be mapped on scales ranging from meters down to a submillimeter to characterize the surface in terms of regolith physical properties, texture, morphology, particle size distribution, and micro- craters. Multispectral imaging will classify and map the compositional heterogeneity of the asteroid's surface in order to spatially support the spectrally resolved information. The study of the spectral slope and albedo will allow to classify the solid surface phases, and to distinguish between carbonaceous, silicates and organic materials. Furthermore, the analysis of color ratios over a given field will provide information on the degree of soil heterogeneity at very small scales. Image series at different sun angles over the course of a day will also contribute to the physical characterization of the asteroid surface properties by photo- metric analysis. The images will also ideally guide the selection of sampling spot(s) of the Hayabusa 2 spacecraft, along with other results from the MASCOT in-situ measurements. Simultaneous observations with the spectrometer and the radiometer of the same surface location will provide comprehensive context information.

Additional imaging during the ballistic hopping and lander relocation mode will allow acquiring meso-scale (resolution: cm) information of the local surface and/or possible indications of horizon glow that cannot be obtained by the orbiter’s imaging system.

The following measurement objectives apply for MasCam:

- investigation of surface features on scales ranging from meters down to a millimeter (regolith physical properties, texture, morphology, microcraters) through descent and close- up imaging, and photometry;
- determination of the rock fragment and particle size distribution of the regolith down to scales in the order of a millimeter;
- Identification of compositional and textural small-scale heterogeneities through color imaging in four spectral channels during dark phases;
- support of the selection of the sampling area by local characterization of candidate sampling sites;
- provide in-situ geological context of the asteroid’s surface as:
    - ground context for orbital measurements of Hayabusa 2
    - context for all other MASCOT in-situ measurements.

2.2.2 MASCOT Geometry

For details of the Mascot coordinate system see the SPICE frame kernel. For an overview see figure 1.

MASCam is mounted inside the MASCOT payload compartment (see figure 1) at the right side (-x direction). The optical axis is oriented towards the bottom (+y, -z direction). The exact values for position and orientation of MASCam can be found in the instrument SPICE kernel and are also included into the PDS4 label of each image file.

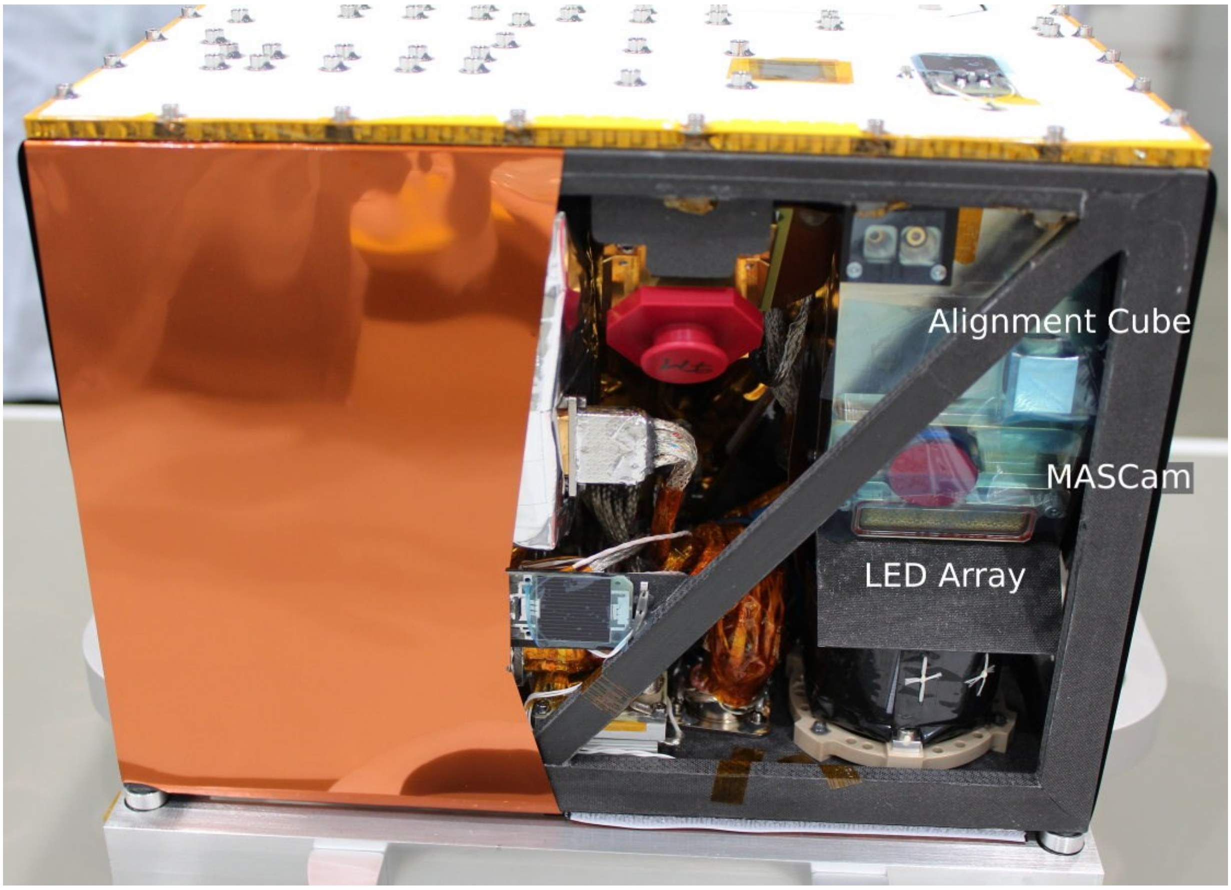

Figure 1: *Image of the +Y side of Mascot, showing some instruments. The +Z axis of the Mascot coordinate system points down, the +X axis points to the left. The center of the Mascot coordinate system is defined as the center of the bottom plane (not visible).*
In this image MASCam is visible to the right (towards the –X direction of Mascot).

2.2.2 Instrument Design and Specifications

For details see the instrument description in [8]. For an overview see figure 2.

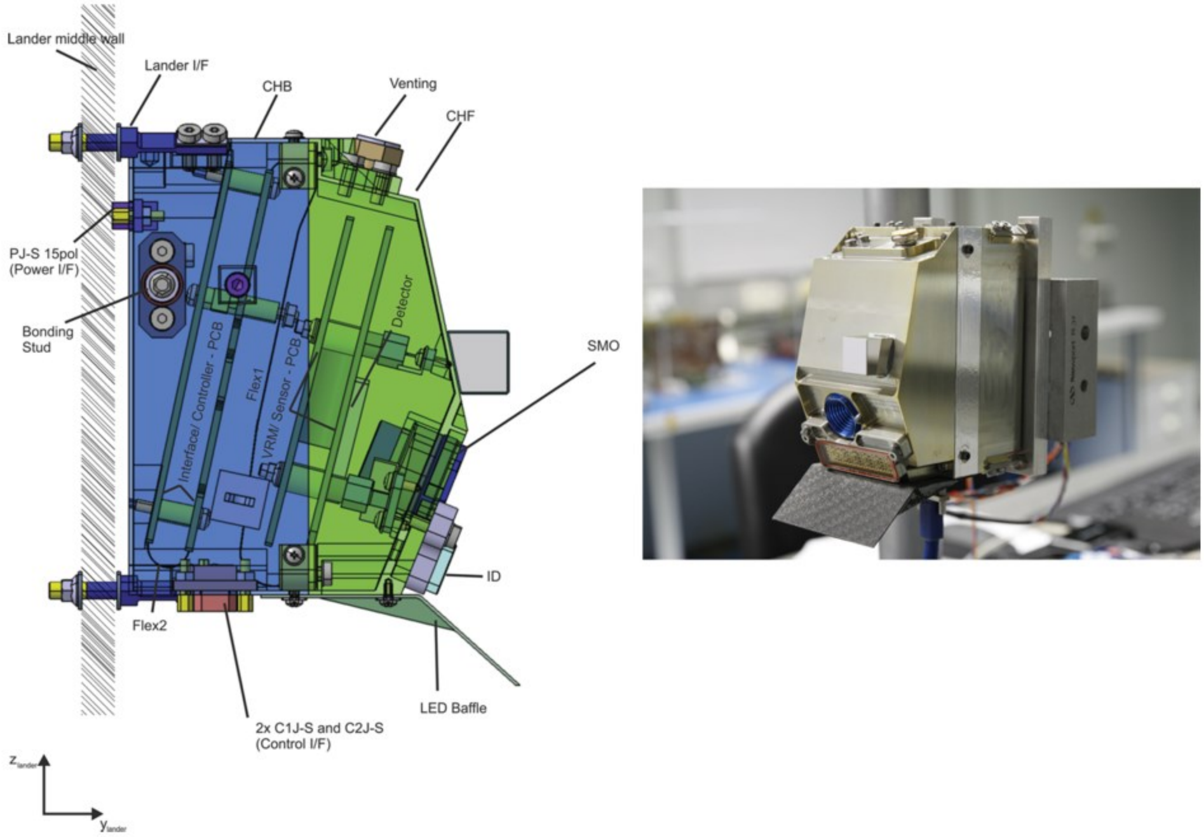

Figure 2: *Left: MASCOT drawing (CHF = Camera Housing Front, CHB = Camera Housing Back SMO = Surface mode optics, ID=Illumination Device, C1J-S,C2J-S,PJ-S = plug definitions). Right: MasCam flight model*

2.2.3 Instrument Operations

For details of the operations during the On-Asteroid phase see [7], included into this bundle.

2.3 Calibration

2.3.1 Geometric Calibration

The results of the ground calibration campaign are described by Jaumann *et al*. [8]. Further investigations of the accuracy of the calibration are included in Schroeder *et al.* [10]. No geometrically calibrated data products are included into this bundle.

2.3.2 Sensor Non-Linearity

The sensor reacts non-linear to light below some threshold, as described by Jaumann *et al*. [8]. This threshold translates to two "critical DN values" (CV) depending on the exposure regime of the camera, i.e. if the exposure time t_{exp} is shorter or longer than 218.8 msec.

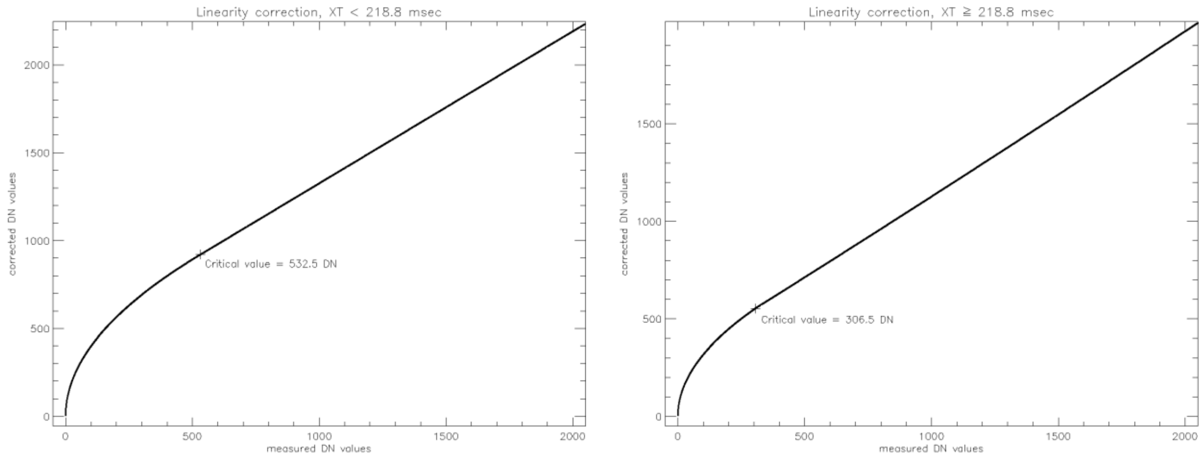

Figure 3: *Non-linearity curves for short (left) and long (right) exposure regime.*

2.3.2.1 Short exposure regime (Exposure Time < 218.8 msec)

CV = 921.5 DN
slope = 0.8654
base_value = 460.8

For measured signals below CV the corrected signal can be calculated as:
corrected_signal = SQRT(4 · slope · base_value · measured_signal)

Otherwise the corrected signal can be calculated as:
corrected_signal = slope · measured_signal + base_value

2.3.2.2 Long exposure regime (Exposure Time ≥ 218.8 msec)

CV = 306.5 DN
a = 0.3055
b = 0.8084
c = 0.01311
base_factor = 1.0016035

kDN = measured_signal / 1000.0

For measured signals below CV the corrected signal can be calculated as:
corrected_signal = 1000 · base_factor · SQRT(kDN)

Otherwise the corrected signal can be calculated as:
corrected_signal = 1000 · (a + b · kDN + c · kDN^2)

2.3.3 Radiometric Calibration

The results of the ground calibration campaign and the resulting radiometric image calibration pipeline are described by Jaumann *et al*. [8]. The health of the camera was verified in-flight through regular Health Check and In-Flight Calibration campaigns (2-3 times per year), in which the camera would acquire images of a calibration target inside of the Hayabusa 2 spacecraft with and without LED illumination. The LED output was found to be stable over time and the temperature was too low (typically around –30° C) to detect dark current. The results of the in-flight calibration campaign did not lead to changes to the radiometric calibration pipeline. We summarize the pipeline as follows, with details provided in [8]. The first step of the radiometric calibration is:

$$\mathbf{C} = [L(\mathbf{W} - \mathbf{B}, t_W) / (t_W - t_B) - f(T_W, T_D) \times L(\mathbf{D} - \mathbf{B}, t_D) / (t_D - t_B)] / \mathbf{F}, \quad (1)$$

where the **C**, **W**, **B**, **D**, **F** are the cleaned, raw, bias, dark, and flat field images, respectively (bold symbols are reserved for images. The exposure times t_W, t_B, and t_D are the exposure times (in [ms]) of the raw, bias, and dark images, respectively. $L(\mathbf{I}, t_{exp})$ is the function that corrects image **I** for non-linearity (as described in 2.3.2.), depending on the exposure time t_{exp}.
The values in the clean image **C** have the unit of [DN/ms^{-1}]. The factor f corrects for the difference in detector temperature of the dark image and the raw image by means of the Arrhenius law:

$$f(T_W, T_D) = \exp[b \times (1/T_D - 1/T_W) / k_B], \quad (2)$$

where b = 1.33×10^{-19} [m^2 kg s^{-2}] and Boltzmann constant $k_B = 1.38065 \times 10^{-23}$ [m^2 kg s^{-2} K^{-1}]. The temperatures in [K] of the raw and dark image are T_W and T_D, respectively.

Factor *f* was generally close to unity. All images were calibrated according to Eq. 1, except bias images, some dark images in night time sets, and sets 2 - 8 and 19.
Bias images **B**, with an exposure time of 0.2138 [ms], were acquired as part of most image sets in Table 1, and were used to calibrate all other images in the set. However, some bias images show "ghosts", artifacts associated with well-illuminated parts of the surface in the previous image. Because stray light from the Sun and MASCOT itself easily dominate the effect of these ghosts, we only replaced the bias image for those sets whose images reveal surface details after strong stretching: To calibrate set 9 we used the bias image from set 8, to calibrate set 11 we used the bias image from set 12 multiplied by a factor of 1.02, to calibrate set 15 we used the bias image from set 14 multiplied by a factor of 1.01, and to calibrate set 16 we used the bias image from set 14 multiplied by a factor of 1.06. Set 1 does not contain a bias image, so we used the bias image from set 14.
Dark exposures **D** were only acquired during the night, and only images from the second night were corrected for dark current (sets 12-14). Because the dark image from set 15 actually shows some illuminated surface in the top right corner, the images in that set were not corrected for dark current. This actually increased the signal-to-noise, as the temperature was low enough to make dark current negligible.
An additional step completes the calibration of images in the second night that were acquired with LED illumination (sets 12-15). The absolute radiometric calibration of these images was extended to radiance:

$$\mathbf{I}_i = (\mathbf{C}_i - \mathbf{S}_i) / (R_i \times \mathbf{V}_i), \quad (3)$$

for each of the four LED colors $i = (1, 2, 3, 4)$ for (Blue, Green, Red, IR). **I** is the radiance image with units of [W / m^2 / sr], **C** the clean image from Eq. 1, *R* the responsivity factor in [m^2 sr mJ^{-1}] (Table 1), **S** the stray light image, and **V** the color ratio image. A modification in Eq. 3 with respect to the version in [2] is the subtraction of a stray light image **S**. It was observed on Ryugu that activating the LEDs caused stray light in the images, which was not seen in test images acquired before launch. The dark sky images acquired during the first night on Ryugu were a blessing in disguise, as they allowed to characterize this stray light. Figure 4 shows the stray light patterns for each LED color as constructed from the images in sets 7 and 8. Stray light can be recognized as a narrow column of signal extending from the image center to the top of the frame, but is also present, more diffusely, in the image corners. It is especially strong for the Blue LED. Dividing by the (normalized) color ratio image **V** corrects for the different illumination patterns for the different LED colors. The ratio images (Figure 5) were derived prior to launch from images of a flat, white plate in the nominal landing orientation. We used the Green pattern as reference, so $\mathbf{V}_2 = \mathbf{1}$, the unity matrix. The actual illumination patterns depend on the scene and were different on Ryugu, but using the patterns in Figure 5 provides a first order correction.

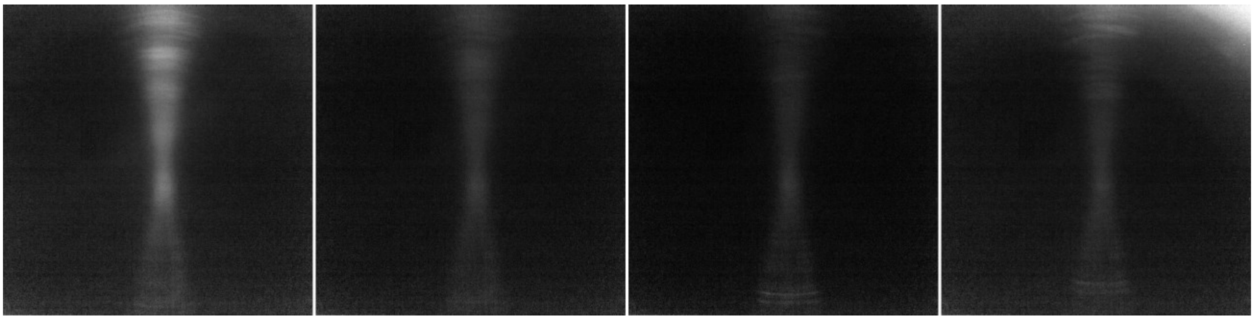

Figure 4: *LED stray light images displayed on the same intensity scale. From left to right: Blue (*$\mathbf{S}_1$*), Green (*$\mathbf{S}_2$*), Red (*$\mathbf{S}_3$*), and IR (*$\mathbf{S}_4$*).*

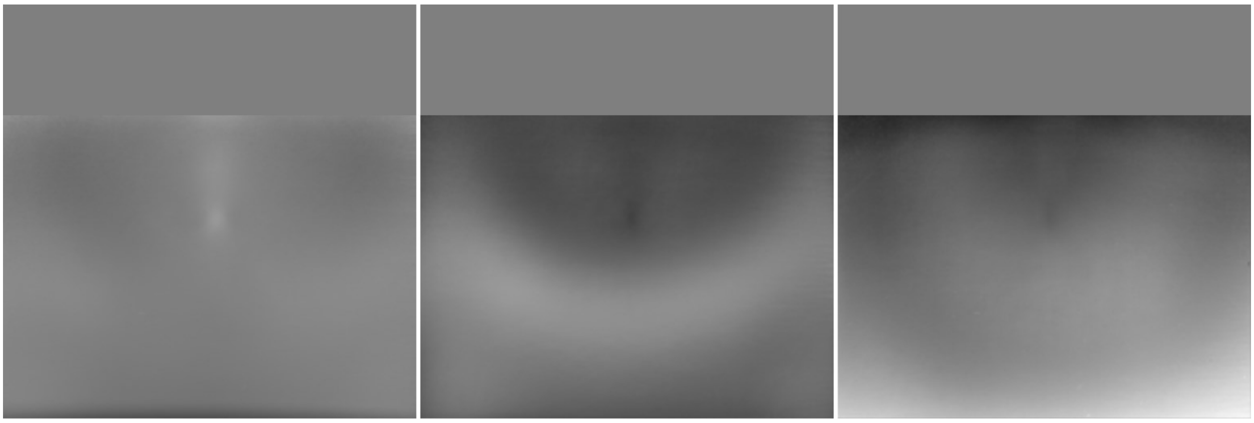

Figure 5: *LED ratio images. Left: Blue over Green ratio image (*$\mathbf{V}_1$*). Middle: Red over Green ratio image (*$\mathbf{V}_3$*). Right: IR over Green ratio image (*$\mathbf{V}_4$*).* $\mathbf{V}_2$ *is the unity matrix. The brightness of the ratio images as displayed is such that 0.7 is black and 1.3 is white.*

2.3.4 Calibration to reflectance

Several MASCAM images show a close-up view of a rock on Ruygu. The night time images of that rock that were calibrated to radiance with Eq. 3 (sets 12-15) can be further calibrated to reflectance (radiance factor, *I/F*) as:

$$\mathbf{R}_i = \pi\ \mathbf{I}_i / J_i, \qquad (4)$$

with the LED irradiance

$$J_i = J_{i,\mathrm{ref}} \times (d_{\mathrm{ref}} / d)^2. \qquad (5)$$

The LED reference irradiance J_{ref} in [W m^{-2}] is defined at a distance of d_{ref} = 20 cm. The actual irradiance depends on the distance *d* (in cm) to the rock and is therefore different for each image pixel. The distance can be derived from a shape model of the rock [9]. We did not calibrate the MASCAM images to reflectance and provide the reference irradiances in Table 1 as a service to the user.

i	LED	λ_{cen}	λ_{eff}	FWHM	*R*	J_{ref}
1	Blue	465	471	455-477	110.7±1.1	2.96±0.09
2	Green	523	532	508-544	129.3±1.2	2.86±0.09
3	Red	633	630	623-640	125.1±1.3	3.55±0.11
4	IR	812	809	792-827	97.1±1.1	1.42±0.04

Table 1. *Radiometric properties of MASCAM LEDs. Wavelength λ and full-width-at-half-maximum (FWHM) are in [nm]. R is the responsivity factor in [m^2 sr mJ^{-1}] and J_{ref} the LED irradiance in [W m^{-2}] at a reference distance of d_{ref} = 20 cm.*

3 MASCam Data Products

3.1 Data Product Overview

During its 17 hour mission at Ryugu, MASCAM acquired 19 sets of images with a total of 120 images, as shown in the overview in Table 2. Each set resulted from the execution of a pre-programmed sequence. Representative images (or image products) for each set are shown in Fig. 5. The details of the imaging sequences are described in the MASCAM activity planning report [7], archived along with this document. Each image received an identifier (GID) as specified by the sequences. The imaging plan was highly robust. The

circumstances surrounding the landing on Ruygu led the camera to skip some sequences described in [7], and repeat others. Because of the repetition, image identifiers are not unique, and images must be identified from the time stamp in the file name. The onboard illumination device, an array of LED in 4 colors, was used in all *Day* and *Night* sequences, just in case the surface in front of the camera was in shadow. It was not used in the *Descent*, *Upright1*, and *Phot* sequences.
We briefly describe the image contents here. Set 1 contains images acquired during the descent of MASCOT to the surface of Ryugu, including the bouncing phase. They show the surface at various spatial resolutions and perspectives. Some show the empty sky, occasionally with the Sun in the field-of-view (FOV). The presence of the Sun in or near the FOV invariably produced stray light. Sets 2 and 3 contain one image each, acquired while the probe attempted to upright. They presumably show the surface below the spacecraft, which was in the shadow. The uprighting was not executed properly, so, after settling, set 4 was acquired with the spacecraft upside-down and the camera looking upward. The Sun was in the FOV, leading to overexposed images with abundant stray light. Sets 5-8 were acquired during the first night on the asteroid and show the dark sky, instead of LED light reflected off the surface. Set 9 was acquired in the early morning of the second day, and the images show some surface in addition to stray light from the Sun, evidence of involuntary spacecraft movement between set 8 and 9. The spacecraft relocated on the morning of the second day and ended up with the correct orientation. Set 10 was acquired during the afternoon, and the images show the surface of Ryugu illuminated by sunlight and light reflected off the metal foil covering the spacecraft. Set 11 was acquired in the evening, and the images show both LED-illuminated surface at the bottom and Sun-illuminated surface at the top of the frame. Sets 12-14 were acquired during the second night and show the surface in LED light. Set 15 was the last one of the night, and the images shows small parts of the surface being illuminated by the Sun in the top right corner. Set 16 was acquired in the early morning of the third day, and the images show both LED-illuminated surface at the bottom and Sun-illuminated surface at the top of the frame in addition to abundant stray light. The spacecraft performed a mini-move in the morning of the third day. The following sets, 17 and 18, show the surface of Ryugu illuminated by sunlight and light reflected off the metal foil covering the spacecraft. Because of involuntary movement between the two sets, the viewing angle was slightly different. The spacecraft relocated in the afternoon, after which MASCAM acquired the last image of the mission; set 19 contains a single image showing only empty sky with stray light.

Asteroid time	**Set #**	**Sequence**	**GID**	**# of images**
Day 1	1	*Descent*	100-119	20
	2	*Upright1*	150	1
	3	*Upright1*	150	1
	4	*Day1_Seq1*	200-207	8
Night 1	5	*Night1_Seq1*	350-355	6
	6	*Night1_Seq2*	400-405	6
	7	*Night1_Seq3*	450-455	6
	8	*Night1_Seq3*	450-455	6
	9	*Night1_Seq3*	450-455	6
Day 2	10	*Day2_Seq2*	600-607	8
Night 2	11	*Night2_Seq1*	650-655	6
	12	*Night2_Seq2*	700-705	6
	13	*Night2_Seq3*	750-755	6
	14	*Night2_Seq3*	750-755	6
	15	*Night2_Seq3*	750-755	6
Day 3	16	*Day3_Seq1*	800-807	8
	17	*Day3_Seq1*	800-807	8
	18	*Day3_Seq2*	850-854	5
	19	*Phot*	300	1

Table 2. *MASCAM data acquired during the mission at Ryugu in chronological order. "Sequence" refers to the name in the activity planning report [7]. The GID is the ground identification number of the images.*

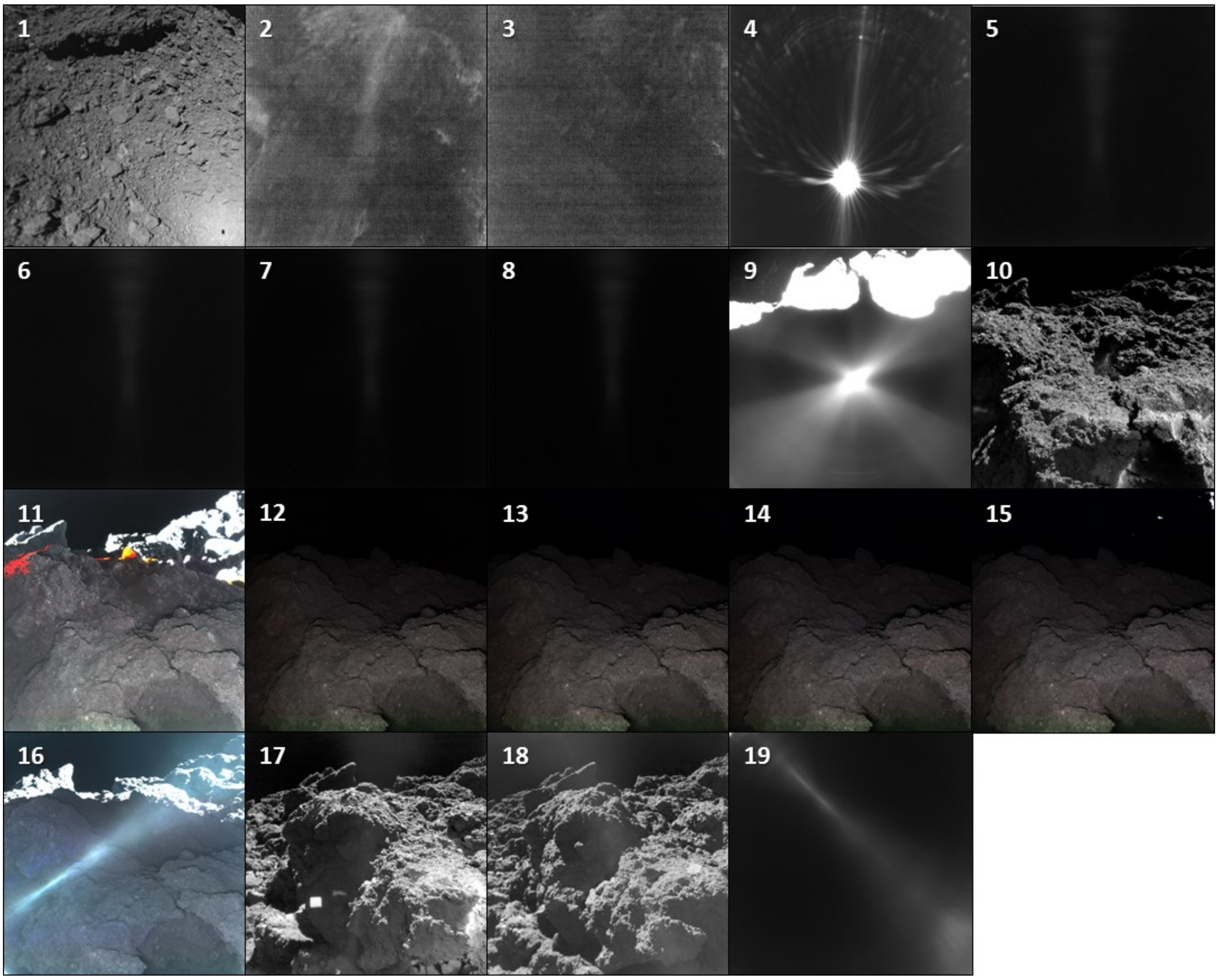

Figure 6. *Representative enhanced images or image products from each set in Table 2, with set number indicated.*

3.2 Data Processing

3.2.1 Data Processing Levels

This bundle contains MASCam data of two processing levels:

- Raw data
- Calibrated data

The calibrated data can be either an only radiometrically cleaned image (i.e. the result of Eq. 1 in 2.3.3, the unit is [DN]), or a radiometrically calibrated plus converted to radiance image (i.e. the result of Eq. 3 in 2.3.3, the unit is [W/m²/sr]).
The state of the calibration for each image can be found in Mascam_Timetable.pdf and by inspecting the label keyword “<unit>”.

3.2.2 Data Product Generation

The MASCam saved the image uncompressed in its internal memory. The image information was then transferred to the MASCOT onboard computer. The MASCOT onboard computer divided the 1024x1024 x16 bit pixel image into 64 tiles with a size of 128x128x16 bit pixels each. These tiles were compressed using wavelet compression and stored for the next transmission to HAYABUSA 2.
The tiling of the image information served the purpose to reduce the loss of data from the entire image if a data packet would be lost during the transfer from the surface to HAYABUSA 2. Fortunately, no such data loss occurred.
After the transfer to Earth and then further to DLR the image tile data and accompanying housekeeping data were used to reconstruct the uncompressed images. The resulting products of this process are the raw image data included in this bundle.
After manually selecting worthwhile images, these images were radiometrically calibrated according to the results of the ground-based calibration described in 2.3.3
The calibration files used in this process are listed in the PDS4 label of the calibrated image data files.

3.3 Standards Used in Generating Data Products

MASCam data products and labels comply with Planetary Data System standards, including the PDS4 data model, as specified in applicable documents.

3.3.1 Time Standards

MASCam uses MASCOT on-board time (MOBT) as spacecraft clock time. The spacecraft clock time is converted to UTC using the MASCOT time correlation functions, described in the Technical Note "MASCOT Time Scales" [6], included in this archive.

3.3.2 Coordinate System

All position coordinates are in Ryugu's body-fixed frame as defined in Preusker et al. [5]. The orientation of MASCOT is described as a transformation from the body-fixed frame of Ryugu into the MASCOT coordinate system. The preliminary reconstruction of the position and orientation of MASCOT is described in Scholten et al. [9].

3.3.3 Data Storage Convention

MASCam image data are stored according to the VICAR format standard, which is described in [4].

3.4 Applicable Software

The image data may be read using PDS4 display software (e.g. "pds4viewer", provided by SBN) or distinct VICAR display software (e.g. "xvd", provided by MIPL, see [4]).

3.5 Backups and Duplicates

The Small Bodies Node keeps online copies of each archive product. One copy is the primary online archive copy. Another is a backup copy. Once the archive products are fully validated and approved for inclusion in the archive, another copy of the archive is sent to the National Space Science Data Center (NSSDC) for long-term preservation in a NASA-approved deep-storage facility. The Small Bodies Node may maintain additional copies of the archive products, either on or off-site as deemed necessary according to the Node's backup and disaster recovery plan.

4 MASCam Archive Organization

4.1 File Naming Convention

The amount of data produced by MASCam is relatively small, and all data from the on-asteroid mission phase will be archived in a single folder for both the raw and the calibrated data.

File names of the image data are of the form

mcam_1086241264_103_00203_n_edr.vic

File name component	Component description
mcam	MASCOT instrument Cam
1086241264	Spacecraft clock time (MOBT) at the end of the image acquisition.
103	Ground identification number The GID is descripted in 3.1, Table 2 and in [7].
00203	Exposure time in $^{1}/_{10}$ms unit, i.e. in this case 20.3ms
n	This flag shows which LED was in use to illuminate the scene n = "NONE" r = "RED" g = "GREEN" b = "BLUE" i = "INFRARED"
edr	Identifier for the processing level: edr = raw images rdr = calibrated images
vic	The extension indicates the data format as VICAR image format.

4.2 Collections

The MASCam bundle contains four collections:

Collection	Description
data_raw	Raw image data. Contains all images from the on-asteroid mission phase (see 3.1)
data_calibrated	Calibrated image data. Contains only selected images from the on-asteroid mission phase. Excluded images: • Bias images (For calibration purposes, see 2.3.3.) • Images that don't show the surface of Ryugu. (I.e. the images of the Sets 2 – 8 and 19, see 3.1, Table 2)
calibration	Calibration files (see also 2.3.3). The collection contains three types of calibration files: • Flatfield correction file, independent of active LED illumination: *mascot_mascam_flatfield_fm.cal*

	• Straylight correction files, one for each of the four LEDs: *mascot_mascam_blue_straylight.cal* *mascot_mascam_green_straylight.cal* *mascot_mascam_ir_straylight.cal* *mascot_mascam_red_straylight.cal* • LED illumination pattern correction files, one for each of the four LEDs: *mascot_mascam_blue_over_green.cal* *mascot_mascam_green_over_green.cal* *mascot_mascam_ir_over_green.cal* *mascot_mascam_red_over_green.cal*
document	Documentation. Contains this document, the reference documents [6] and [7], and a document that contains a table of all image products with position, time, and calibration information (*Mascam_Timetable.pdf*).

5 MASCam Archive Product Formats

Data that comprise the MASCam data archive are formatted in accordance with PDS specifications. This section provides details on the formats used for each of the products included in the archive.

5.1 Product Formats

This section describes the format and record structure of each of the data file types.

5.1.1 Image Data Products

All image files (both raw and calibrated) are stored in the VICAR image format.
Metadata for each image can be found in the accompanying XML label file.
These metadata include:

- Time of image acquisition, both in UTC format and in spacecraft clock time
- Active LED
- Exposure duration
- Compression parameters
- Instrument temperature
- Position of Mascot (preliminary values)
- Orientation of Mascot (preliminary values)
- Geometrical model of the camera (CAHV)
- Used SPICE kernels
- Calibration files used (for calibrated images only)

5.1.2 Calibration Files

All calibration files are in the VICAR image format. The accompanying XML label files contain no special metadata.

5.1.3 Document Products

Documents in the MASCam archive are provided as PDF/A.

5.2 PDS Labels

Each MASCam product is accompanied by a PDS4 label. PDS4 labels are ASCII text files written in the eXtensible Markup Language (XML). Product labels are detached from the files they describe (with the exception of the Product_Bundle label). There is one label for every product. A PDS4 label file usually has the same name as the data product it describes, but always with the extension ".xml".

- END OF DOCUMENT -